Thermal properties of dense matter

M. Prakash

Department of Physics & Astronomy
Ohio University, Athens, OH

Friday, May 29, 2015

PALS: C. Constantinou, B. Muccioli, & J.M. Lattimer
Al Mamun, Xilin Zhang

Workshop on Neutron Star Mergers

May 27 - 29, 2015, Thessaloniki, Greece

Topics/Questions to be addressed

Consistency with the EOS used in Heavy-Ion Collisions

- Can the EOS used in heavy-ion collisions support a 2 $\mathrm{M}_{\odot}$ neutron star?

Thermal Properties of Dense matter: The Bulk Homogeneous Phase

- Can we identify physical quantities (possibly accessible to experiments) that control thermal effects?
- The crucial role of the nucleon effective masses.

Thermal Properties of Dense Matter: The Inhomogeneous Phase

- Which state variable is affected the most by light nuclear clusters?
- How do nuclei respond to heat? Influence of collective effects.

Thermal and adiabatic indices

- See talk by Constantinou.

Theoretical Analysis of Heavy-Ion Collisions

$$\frac{\partial f}{\partial t} + \vec{\nabla}_p U \cdot \vec{\nabla}_r f - \vec{\nabla}_r U \cdot \vec{\nabla}_p f =$$
$$- \frac{1}{(2\pi)^6} \int d^3p_2\, d^3p_{2'}\, d\Omega \frac{d\sigma_{NN}}{d\Omega}\, v_{12} (2\pi)^3\, \delta^3(\vec{p} + \vec{p}_2 - \vec{p}_{1'} - \vec{p}_{2'})$$
$$\times \left[f f_2 (1 - f_{1'})(1 - f_{2'}) - f_{1'} f_{2'} (1 - f)(1 - f_2) \right] .$$

$f(\vec{r}, \vec{p}, t)$: Phase space distribution function of a nucleon

$d\sigma_{NN}/d\Omega$: Differential nucleon–nucleon cross section

v_{12}: Relative velocity

$U \equiv U(n, \vec{p})$ = Mean field or the single particle potential

From a Hamiltonian density (EOS) of many-body physics,

$$\epsilon_{ki} = k_i^2 \frac{\partial \mathcal{H}}{\partial \tau_i} + \frac{\partial \mathcal{H}}{\partial n} = \frac{\hbar^2 k^2}{2m} + U_i(n, k)$$

Observables confronted include:

(i) the mean transverse momentum per nucleon $\langle p_x \rangle / A$ versus rapidity y/y_{proj},
(ii) flow angle from a sphericity analysis,
(iii) azimuthal distributions, and (iv) radial flow.

A model with finite-range interactions (MDI)

$$\mathcal{H} = \frac{1}{2m}(\tau_n + \tau_p) + V(n_n, n_p, T)$$

$$\begin{aligned}
V &= \frac{A_1}{2n_0}(n_n + n_p)^2 + \frac{A_2}{2n_0}(n_n - n_p)^2 \\
&+ \frac{B}{\sigma+1}\frac{(n_n + n_p)^{\sigma+1}}{n_0^{\sigma}}\left[1 - y\frac{(n_n - n_p)^2}{(n_n + n_p)^2}\right] \\
&+ \frac{C_l}{n_0}\sum_i \int d^3p_i \; d^3p_i' \; \frac{f_i(\vec{r}_i, \vec{p}_i) f_i'(\vec{r}_i', \vec{p}_i')}{1 + \left(\frac{\vec{p}_i - \vec{p}_i'}{\Lambda}\right)^2} \\
&+ \frac{C_u}{n_0}\sum_i \int d^3p_i \; d^3p_j \; \frac{f_i(\vec{r}_i, \vec{p}_i) f_j(\vec{r}_j, \vec{p}_j)}{1 + \left(\frac{\vec{p}_i - \vec{p}_j}{\Lambda}\right)^2} \quad ; \quad i \neq j.
\end{aligned}$$

Energy spectrum

$$\epsilon_{p_i} = p_i^2 \frac{\partial \mathcal{H}}{\partial \tau_i} + \frac{\partial \mathcal{H}}{\partial n_i} = \frac{p_i^2}{2m} + U_i(n_n, n_p, p_i)$$

$$U_i(n_i, n_j, p_i) = \mathcal{U}_i(n_i, n_j) + R_i(n_i, n_j, p_i) \quad ; \quad i \neq j$$

The momentum dependence is contained in

$$\begin{aligned} R_i(n_i, n_j, p_i) &= \frac{2C_l}{n_0} \frac{2}{(2\pi\hbar)^3} \int d^3p_i' \, \frac{f_{p_i'}}{1 + \left(\frac{\vec{p}_i - \vec{p}_i'}{\Lambda}\right)^2} \\ &+ \frac{2C_u}{n_0} \frac{2}{(2\pi\hbar)^3} \int d^3p_j \, \frac{f_{p_j}}{1 + \left(\frac{\vec{p}_i - \vec{p}_j}{\Lambda}\right)^2} \, . \end{aligned}$$

The leading order density-dependent term is $\propto p_i^2$, which leads to the spectrum of zero-range Skyrme interactions.

Single particle potentials

$$\epsilon_{ki} = k_i^2 \frac{\partial \mathcal{H}}{\partial \tau_i} + \frac{\partial \mathcal{H}}{\partial n} = \frac{\hbar^2 k^2}{2m} + U_i(n,k)$$

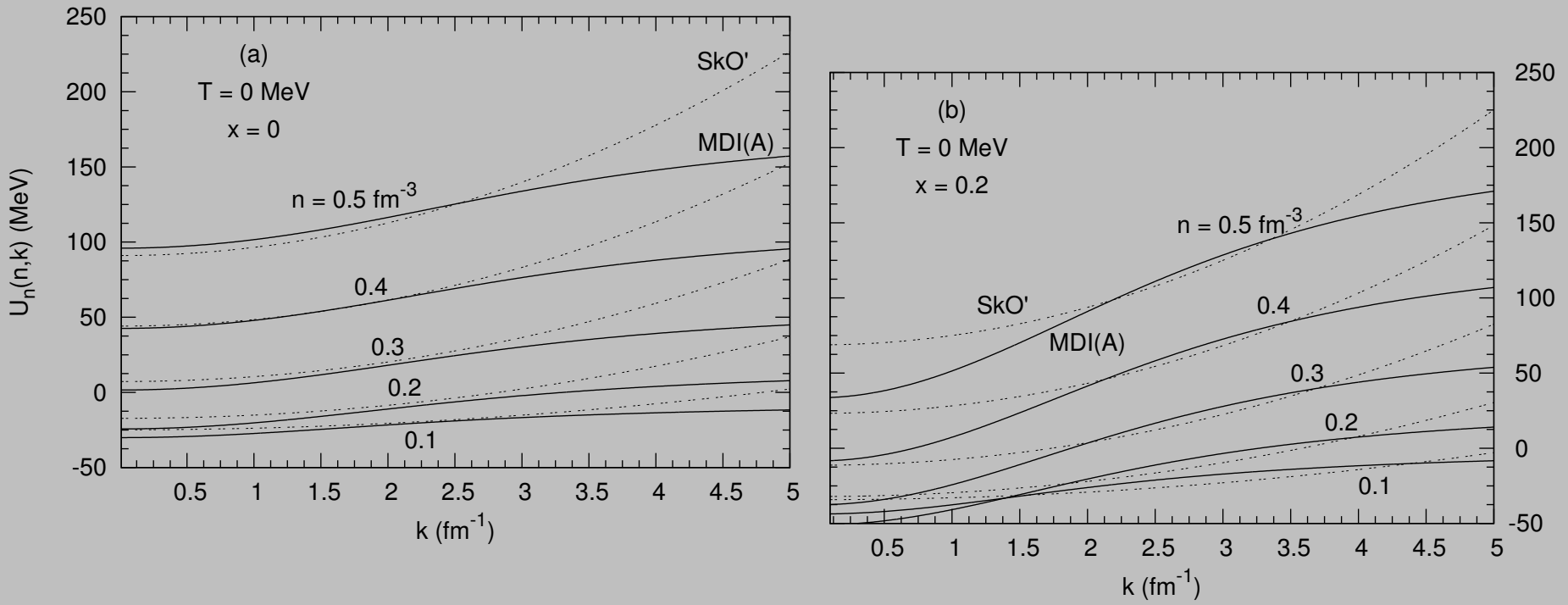

Confrontation with Data

Beam energies: $\frac{E_{lab}}{A} = 0.5 - 2$ GeV

Highest densities reached: $\frac{n}{n_0} = 2 - 3$

Particle detection inefficiencies cause the experimental transverse momenta in the backward direction to be artificially biased towards large negative values and are therefore unreliable.

C. Gale, G.M. Welke, M. Prakash, S.J. Lee, & S. Das Gupta, Phys. Rev. C **41**, 1545 (1989)

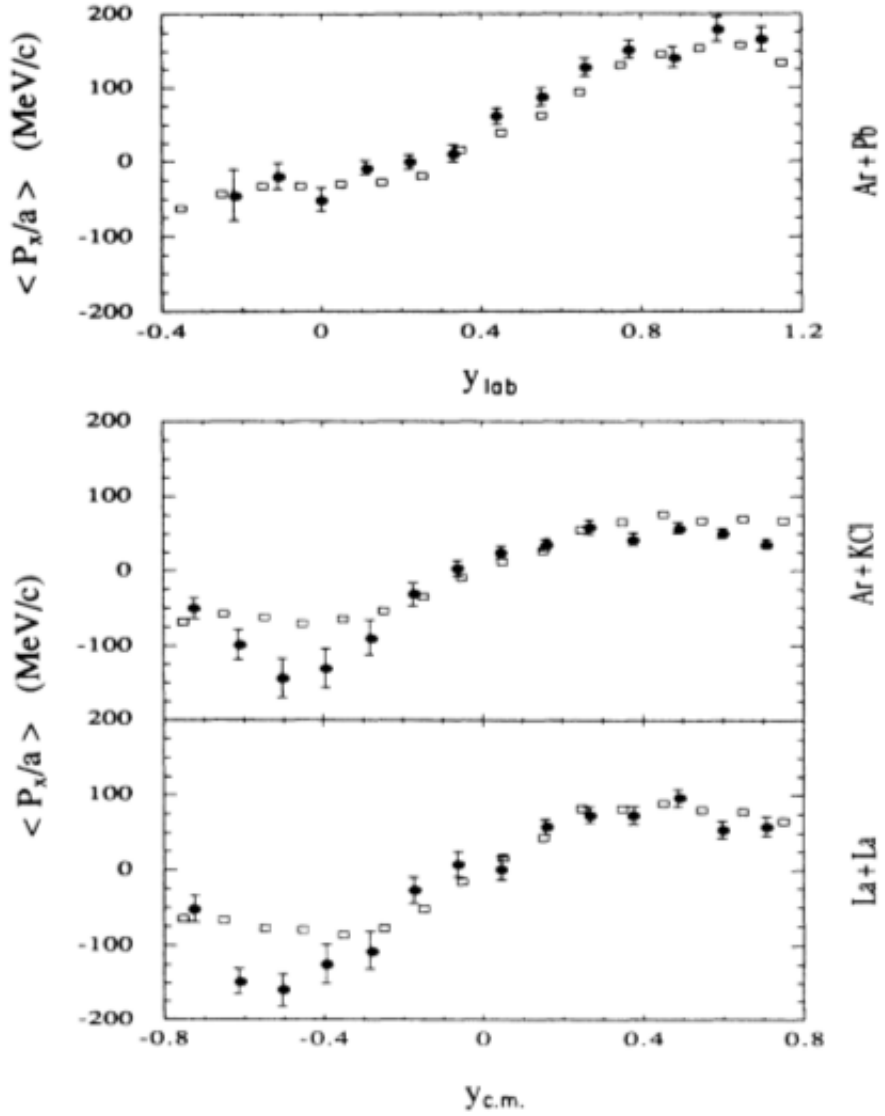

FIG. 10. Transverse momentum per nucleon as a function of rapidity in reactions of 800 MeV per projectile nucleon. Results of BUU simulations with the MDYI interaction (open squares) are compared with the data of Ref. 12 (solid circles). Results for Ar+Pb are in the lab, for La+La and Ar+KCl in the center of mass.

Summary of the EOS from heavy-ion collisions

Zero-range Skyrme models and its variants (that are consistent with the analyses of giant resonances of nuclei with $K_0 = 230 \pm 30$ MeV) give too much sideways flow inconsistent with heavy-ion data. Earlier improper treatments in these models even suggested $K_0 \sim 400$ MeV!

The equation of state implied by the momentum-dependent potential required to fit heavy-ion flow data (and consistent with the analyses of giant resonances of nuclei) is able to support a 2 $\mathrm{M}_\odot$ neutron star.

Thermal properties of EOS's with momentum-dependent forces:

C. Constantinos, B. Muccioli, M. Prakash & J.M. Lattimer, arXiv:1504.03982

Thermal properties & the nucleon effective mass

Landau Fermi Liquid Theory (Degenerate Limit)

- Interaction switched-on adiabatically
- Entropy density and number density maintain their free Fermi-gas forms:

$$s_i = \frac{1}{V}\sum_{k_i}\left[f_{k_i}\ln f_{k_i} + (1-f_{k_i})\ln(1-f_{k_i})\right]$$

$$n_i = \frac{1}{V}\sum_{k} f_{k_i}(T)$$

- $\int d\varepsilon \frac{\delta s}{\delta T} \quad \Rightarrow \quad s_i = 2a_i n_i T$

$$a_i = \frac{\pi^2}{2}\frac{m_i^*}{k_{Fi}^2}$$

level density parameter

Degenerate Limit Thermodynamics

Maxwell's relations:

- Energy density

$$\frac{d\varepsilon}{ds} = T$$
$$\varepsilon(n,T) = \varepsilon(n,0) + \frac{T^2}{n}\sum_i a_i n_i$$

- Pressure

$$\frac{dp}{dT} = -n^2\frac{d(s/n)}{dn}$$
$$p(n,T) = p(n,0) + \sum_i \left[a_i n_i - n\frac{d(a_i n_i)}{dn}\right] T^2$$

- Chemical potentials

$$\frac{d\mu}{dT} = -\frac{ds}{dn}$$
$$\mu(n,T) = \mu(n,0) - T^2\left[\frac{a_i}{3} + \sum_j \frac{n_j a_j}{m_j^*}\frac{dm_j^*}{dn_i}\right]$$

- Free energy density

$$\frac{d\mathcal{F}}{dT} = -s$$
$$\mathcal{F}(n,T) = \mathcal{F}(n,0) - \frac{T^2}{n}\sum_i a_i n_i$$

Nucleon effective masses in models - I

Landau effective masses:

$$m_i^* \equiv \hbar^2 k_{Fi} \left(\left. \frac{\partial \epsilon_{ki}}{\partial k} \right|_{k_{Fi}} \right)^{-1}, \qquad i = n, p$$

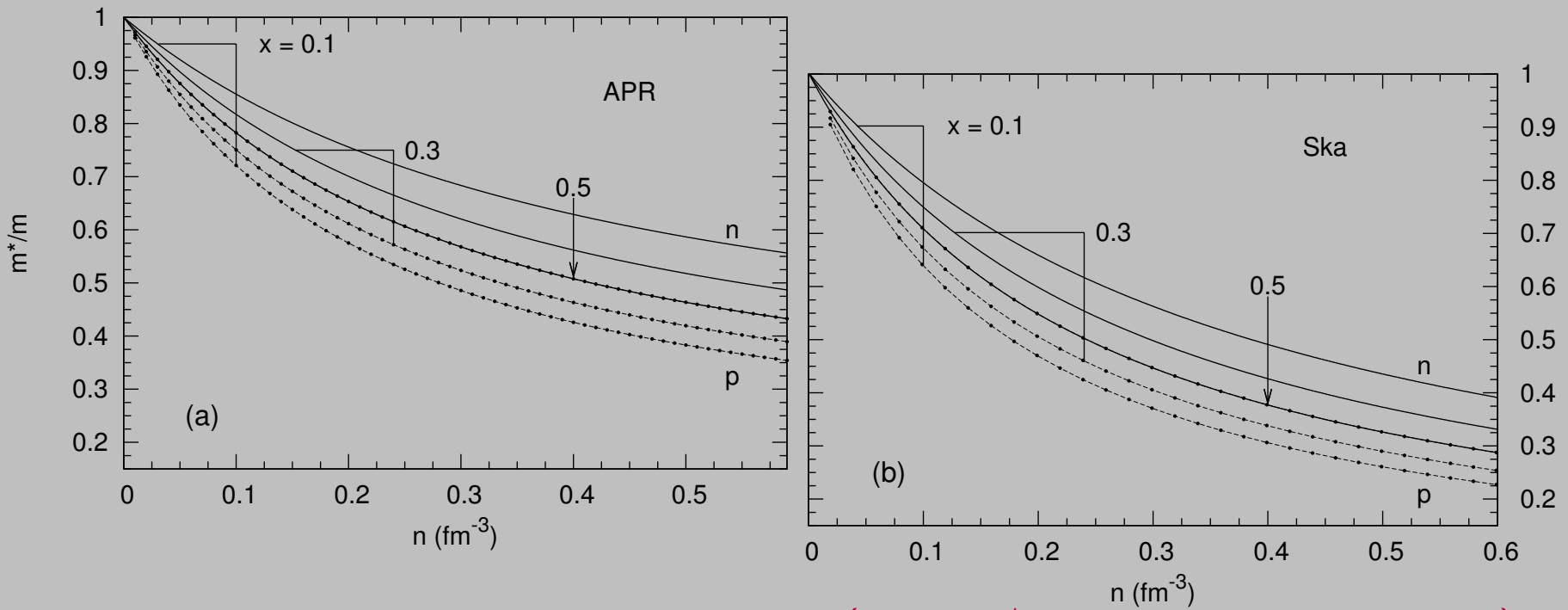

Note the isospin dependence of m^*'s ($x = n_p/n_b$ is the proton fraction). Several Skyrme models exhibit the opposite trend (that is, $m_p^* > m_n^*$ for all x and n). For thermal properties of the APR model, see C. Constantinos, B. Muccioli, M. Prakash & J.M. Lattimer, Phys. Rev. C **89**, 065802 (2014).

Nucleon effective masses in models - II

Landau effective masses:

$$m_i^* \equiv \hbar^2 k_{Fi} \left(\left. \frac{\partial \epsilon_{ki}}{\partial k} \right|_{k_{Fi}} \right)^{-1}, \qquad i = n, p$$

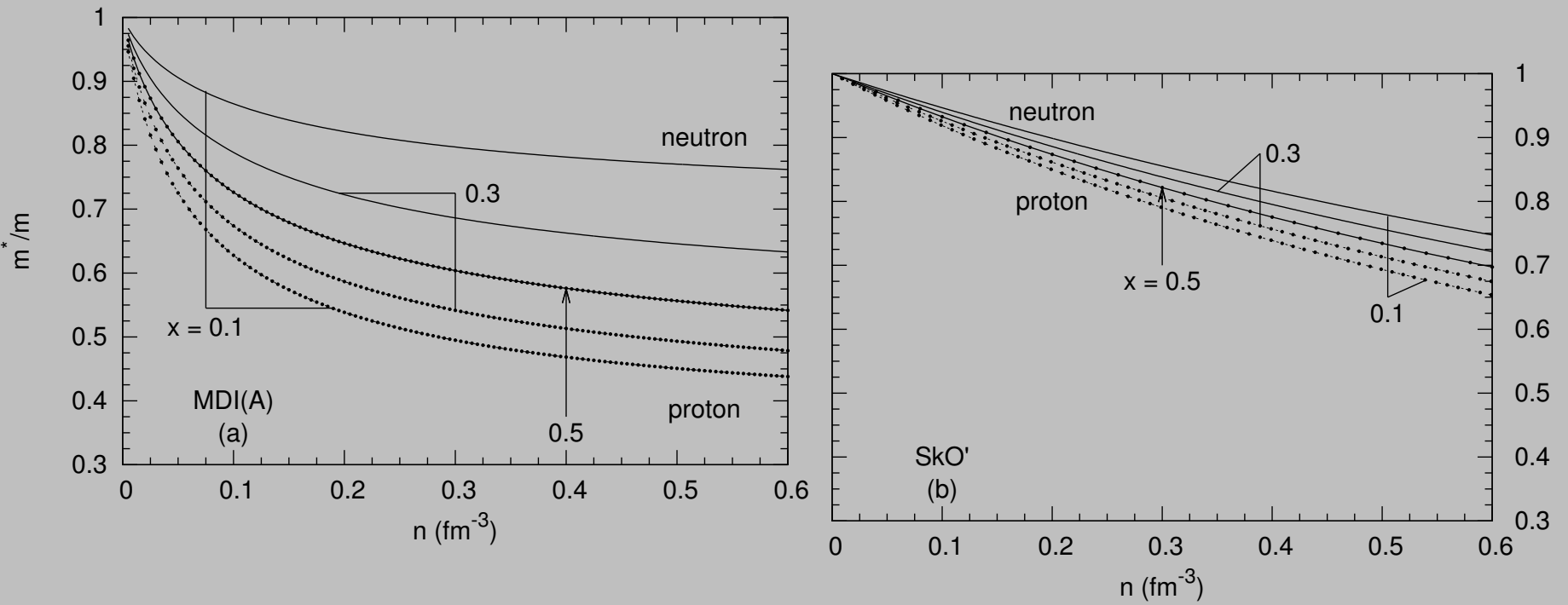

MDI m^*/m's level off with n more rapidly than those of Skyrme models.

Zero Temperature Energy and Pressure

Insets: Results for charge-neutral and β-equilibrated neutron-star matter.

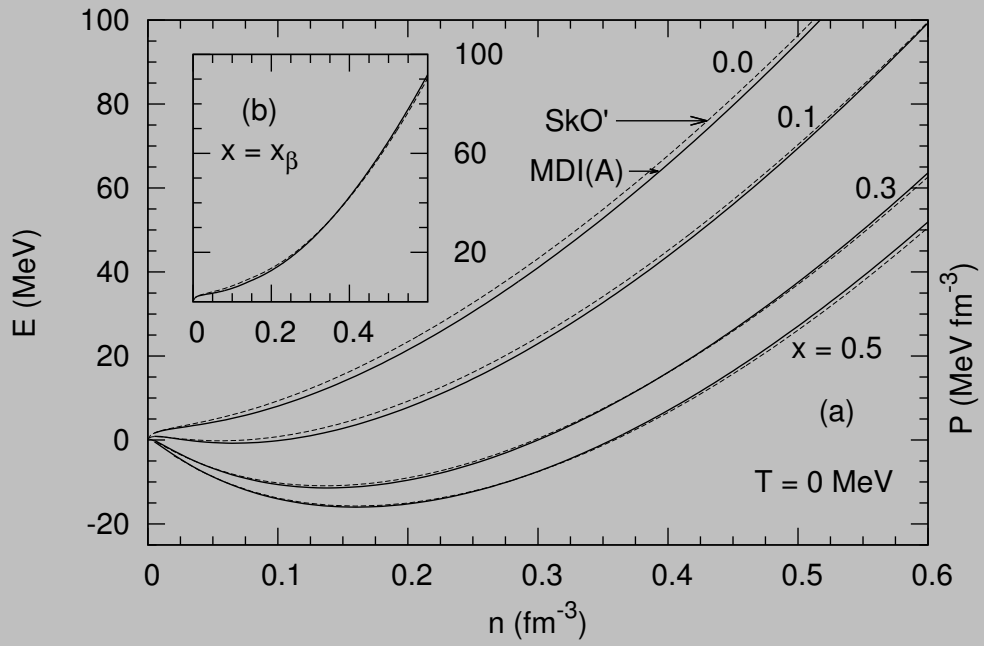

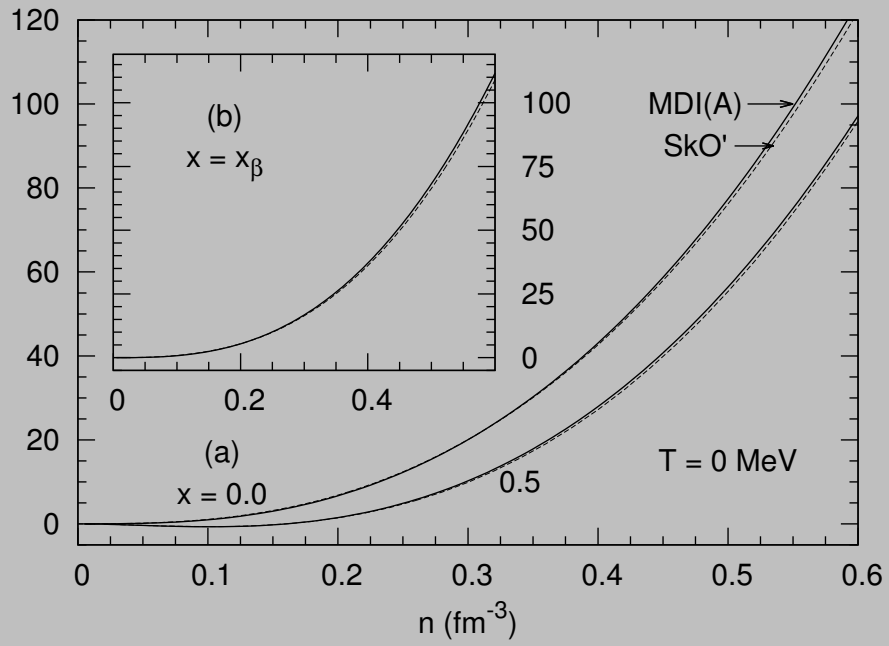

The two models give nearly identical results.

Symmetry energies

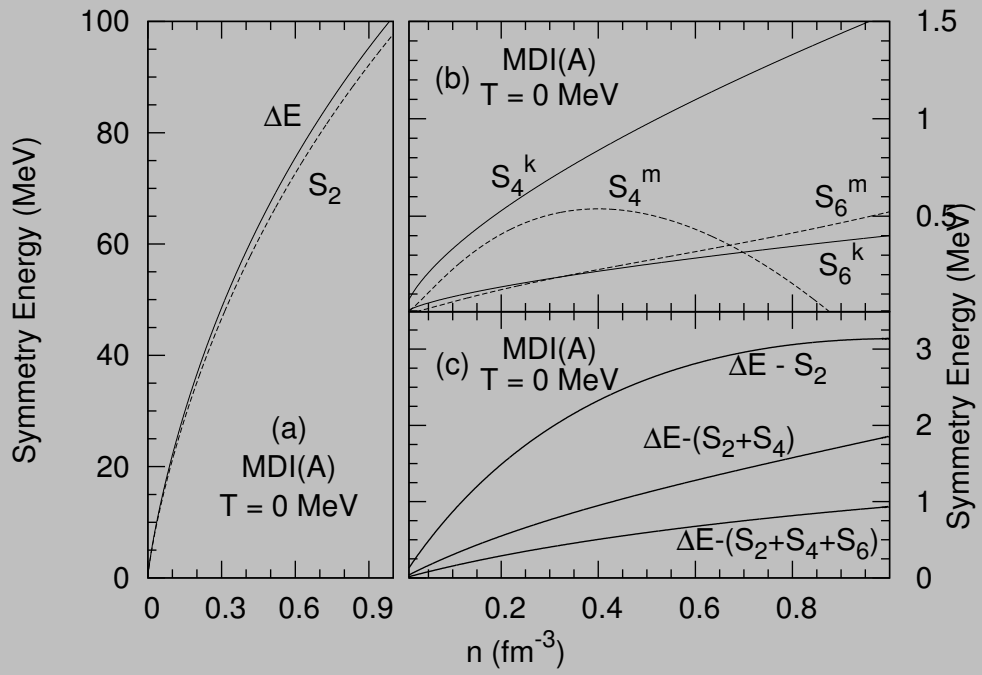

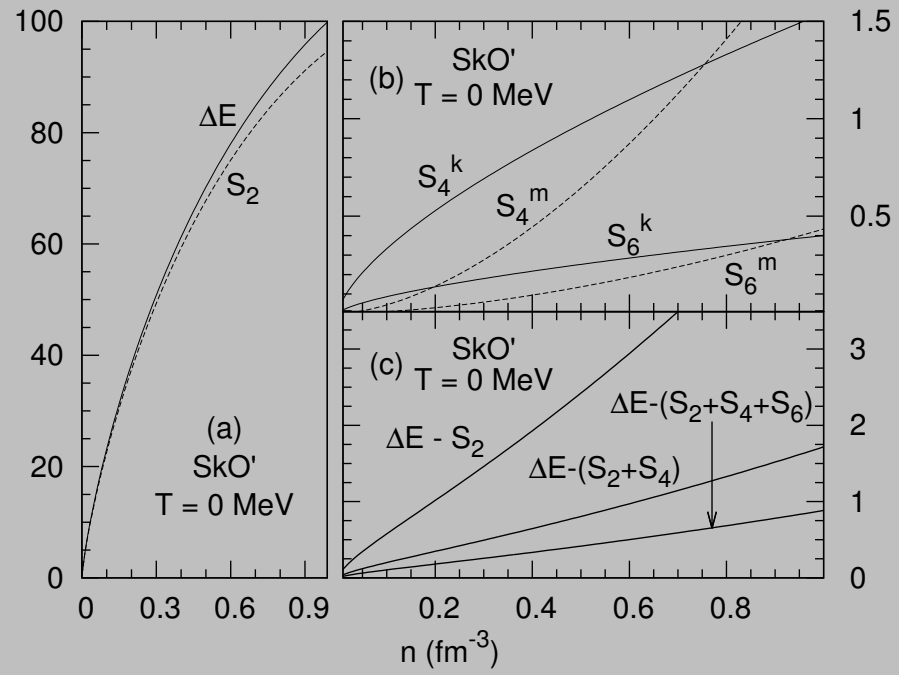

Some differences in the convergence properties of

$$S_I = \frac{1}{\ell!}\frac{\partial^\ell(n,\alpha)}{\partial\alpha^\ell} \qquad \ell = 2, 4, \ldots$$

Neutron star attributes

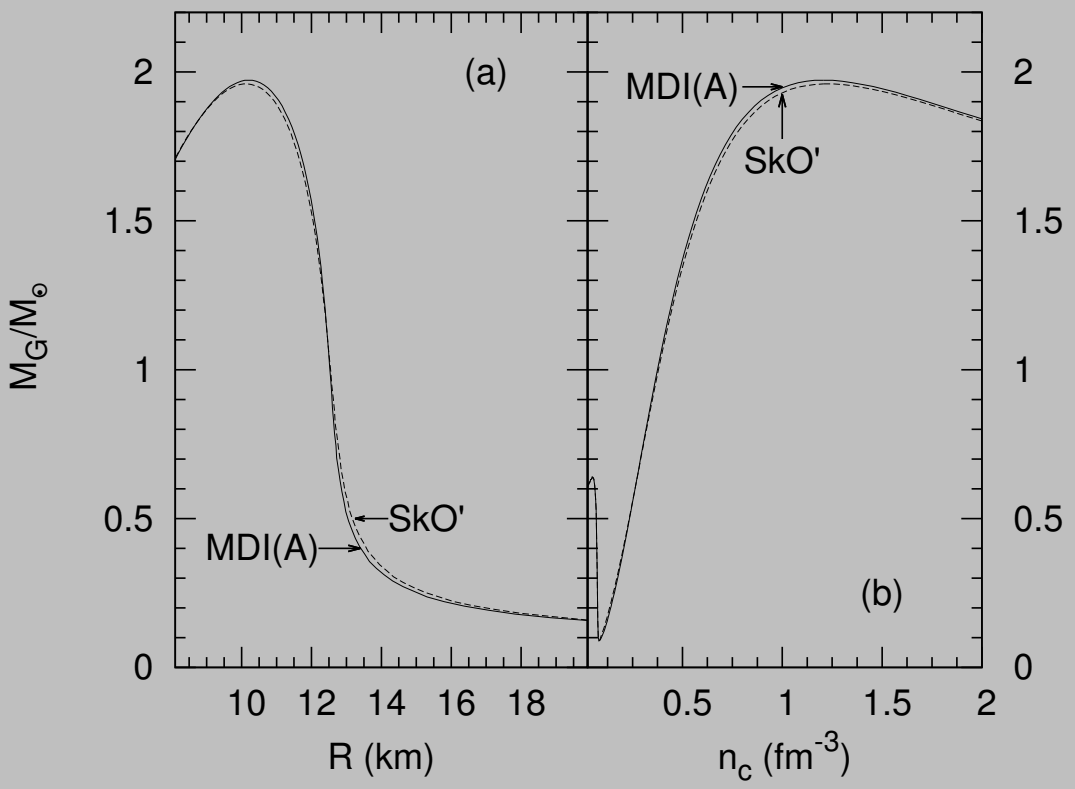

- Direct Urca thresholds:
- MDI(A): 0.67(0.93) fm^{-3} for $e^-(e^- + \mu^-)$
- Corresponding masses: $> 1.7(1.9)\mathrm{M}_\odot$
- SkO′: 0.59(0.92) fm^{-3} for $e^-(e^- + \mu^-)$
- Corresponding masses: $> 1.5(1.9)\mathrm{M}_\odot$

The two models give nearly identical results. Larger masses ensue with minimal changes in the stiffness (e.g., K_0) at near nuclear densities.

Thermal energy and pressure

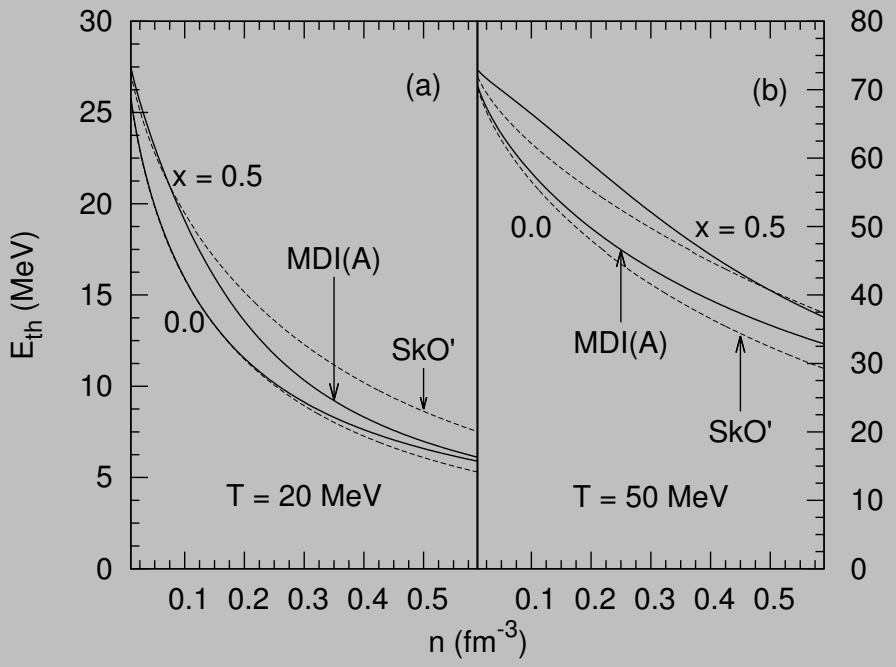

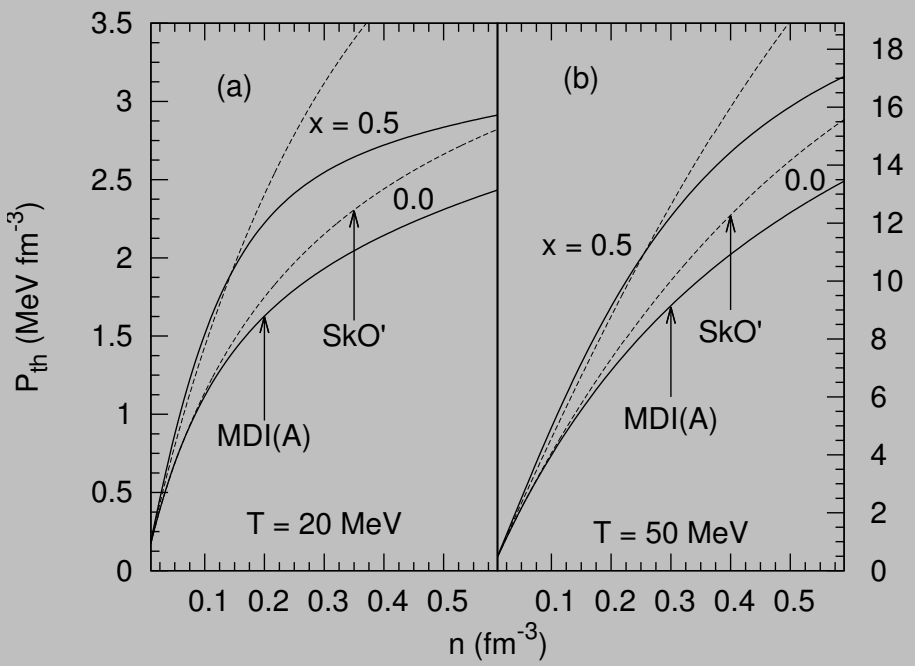

Qualitative trends are similar for the two models.
Quantitative differences are T and x (proton fraction) dependent.

Entropy and specific heat at constant volume

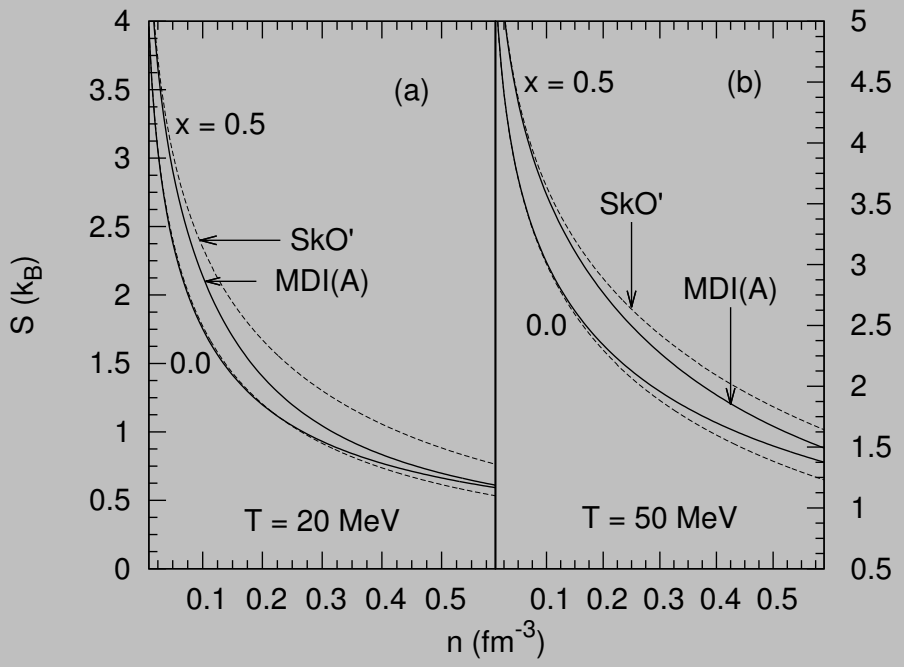

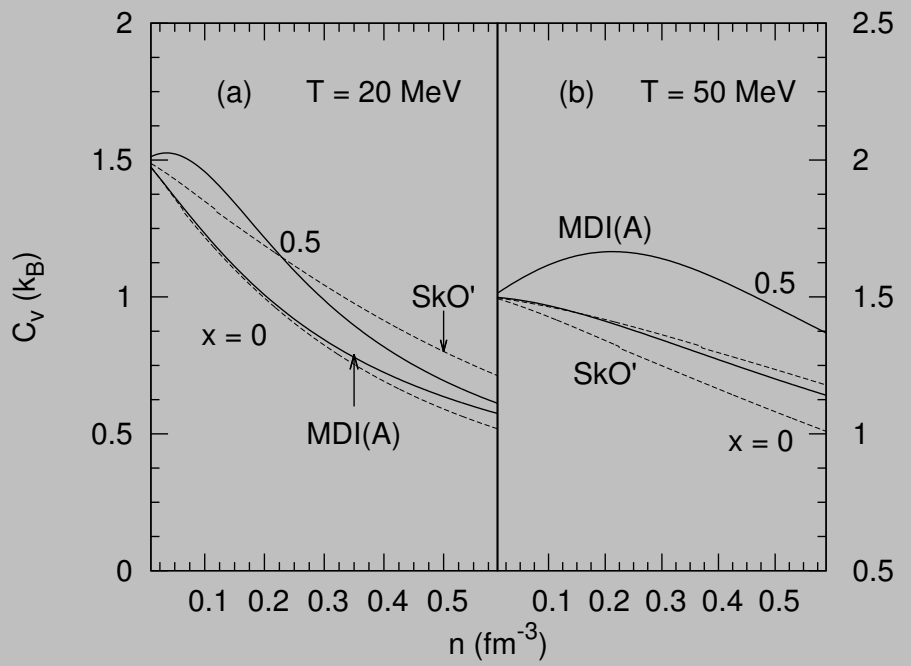

Qualitative trends are similar for the two models.
Quantitative differences are T and x (proton fraction) dependent.

Specific heat at constant pressure and C_P/C_V

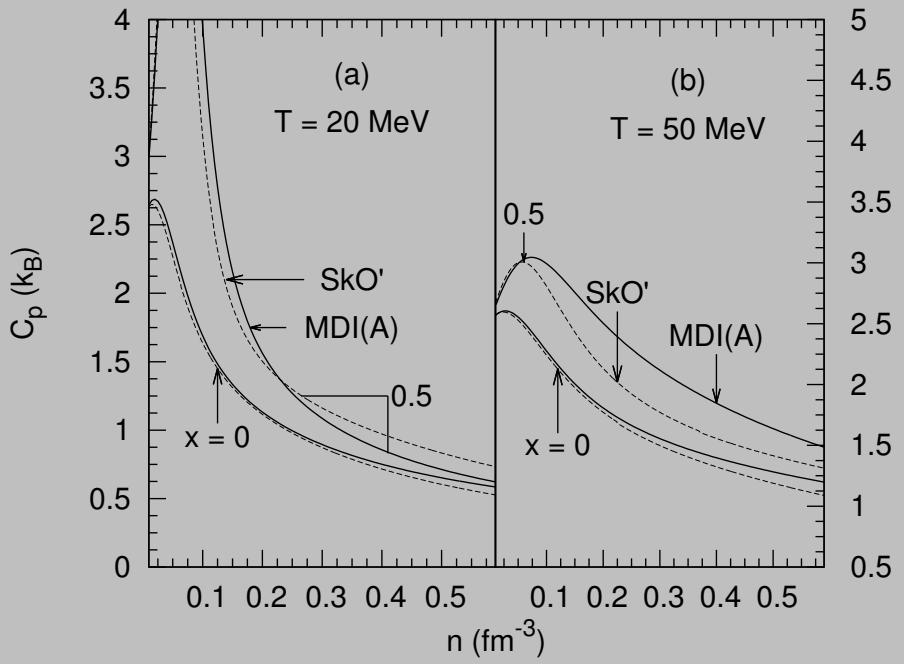

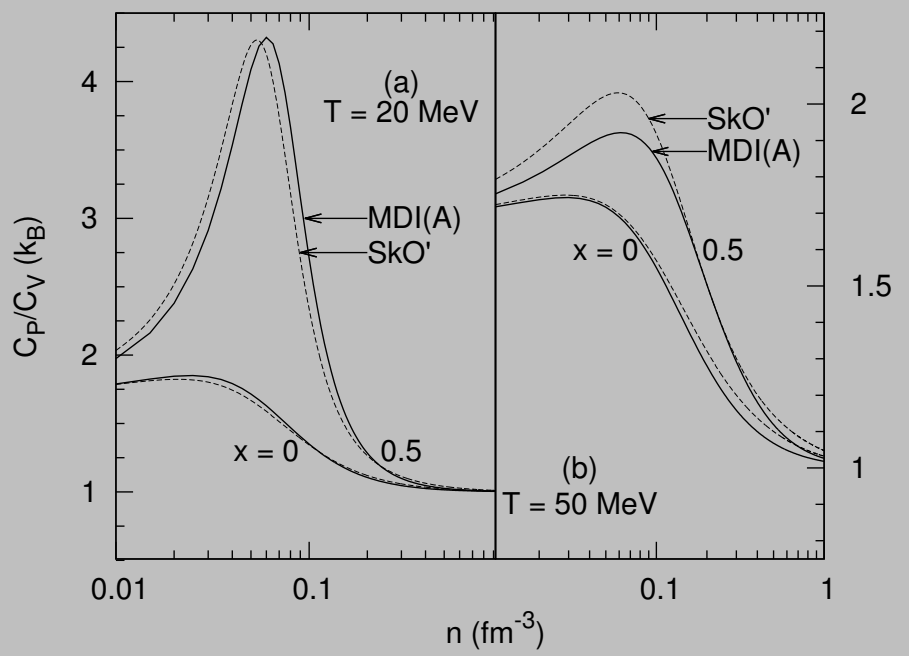

Qualitative trends are similar for the two models.
Quantitative differences are T and x (proton fraction) dependent.

Comparisons in special limits (E_{th})

Analytical expressions delineate the degenerate (Deg.) and non-degenerate (Non-Deg.) regions as well provide checks on exact numerical calculations.

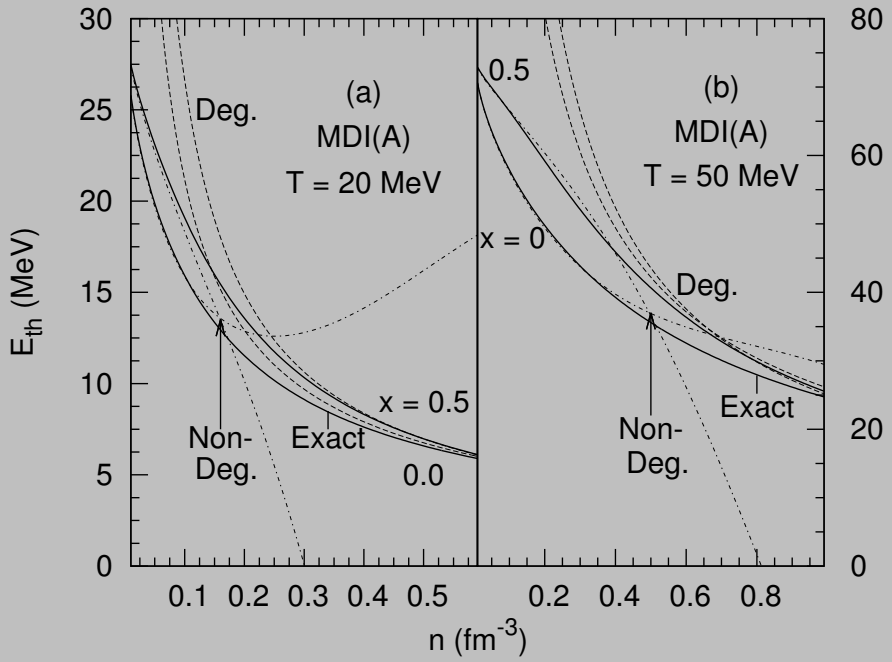

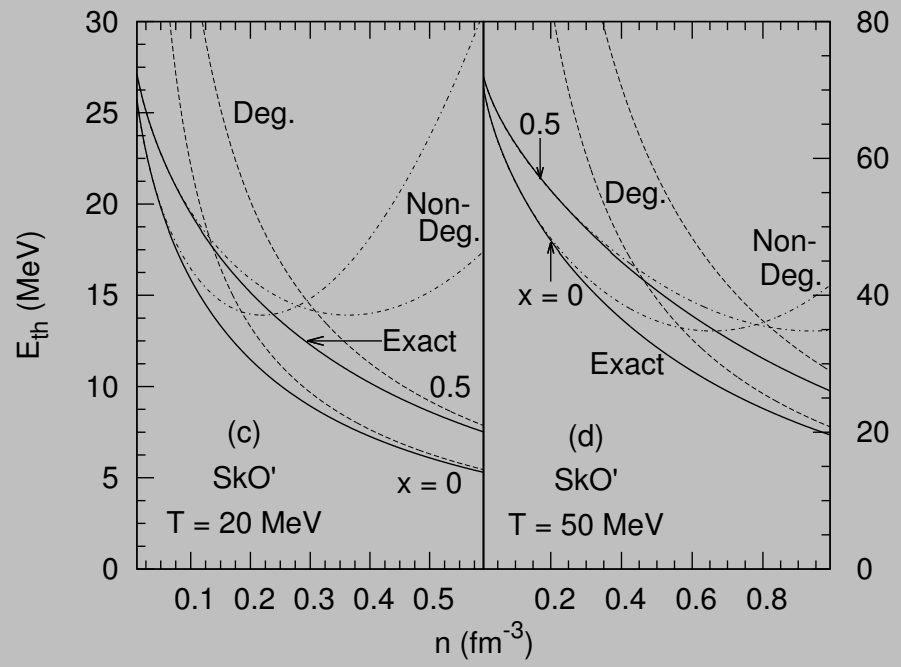

Quantitative differences are T and x (proton fraction) dependent.

Comparisons in special limits (P_{th})

Analytical expressions delineate the degenerate (Deg.) and non-degenerate (Non-Deg.) regions as well provide checks on exact numerical calculations.

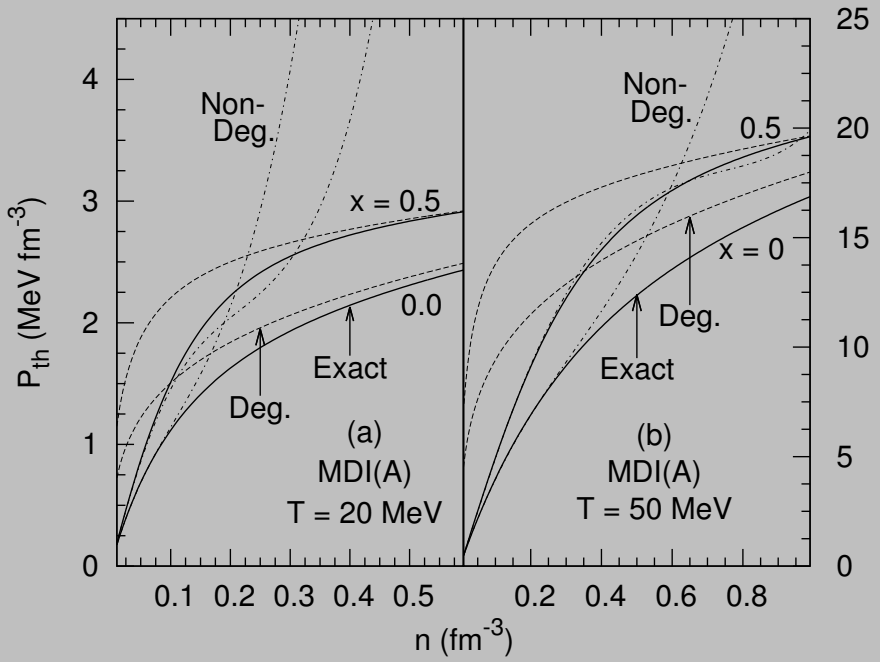

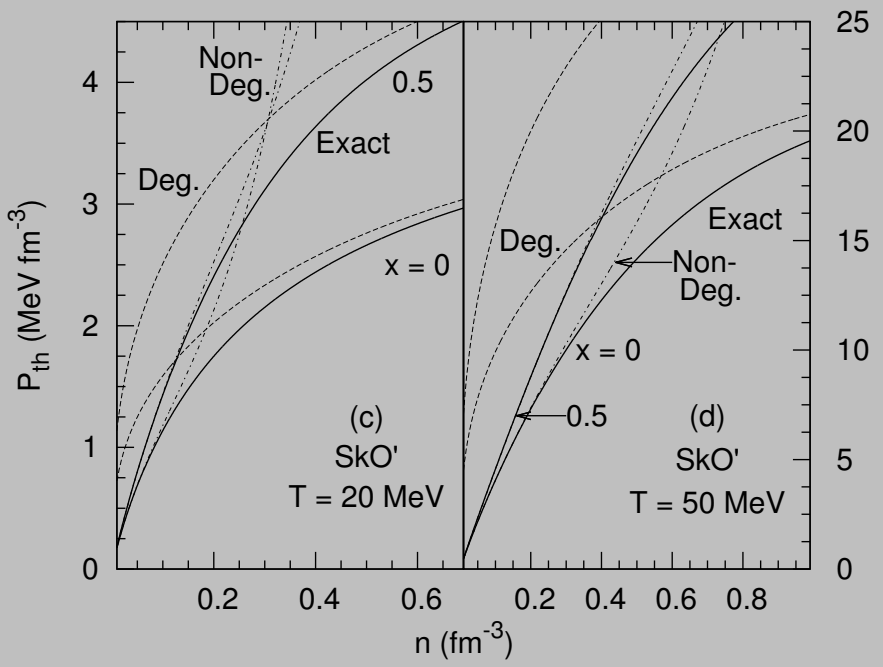

Quantitative differences are T and x (proton fraction) dependent.

Comparisons in special limits (S)

Analytical expressions delineate the degenerate (Deg.) and non-degenerate (Non-Deg.) regions as well provide checks on exact numerical calculations.

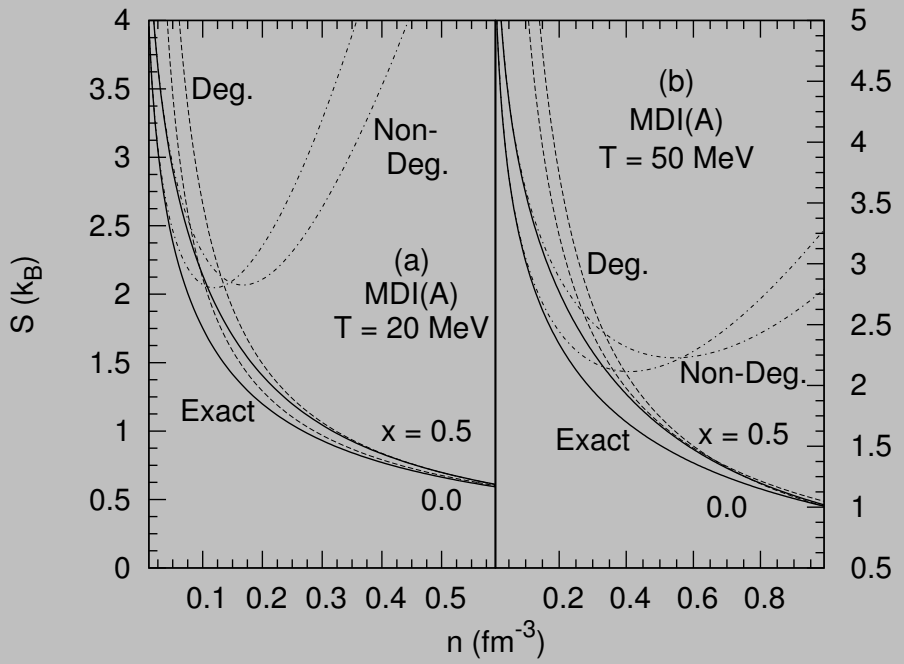

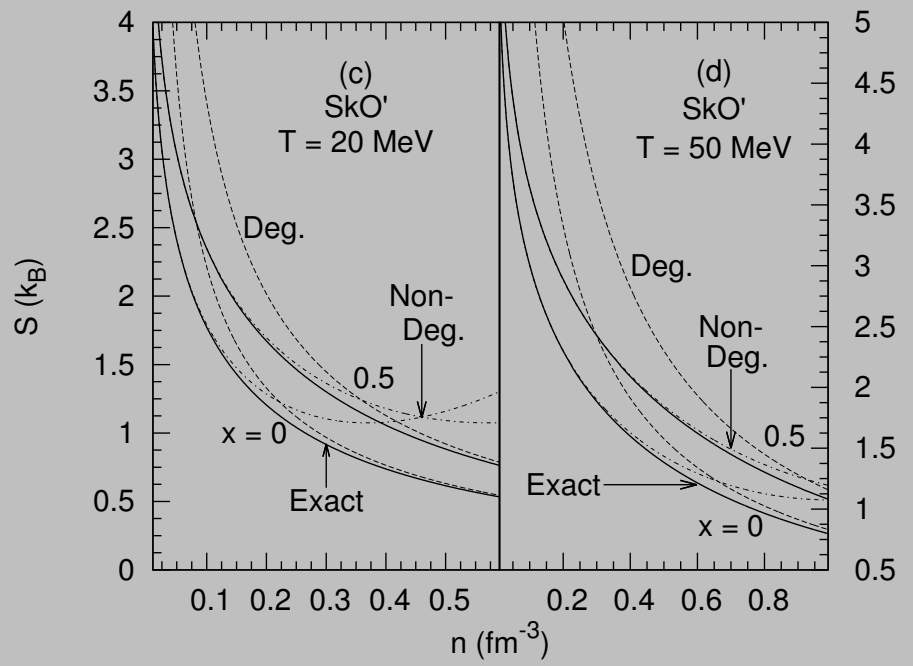

Quantitative are differences T and x (proton fraction) dependent.
Different state variables exhibit different rates of convergence.

Comparisons in special limits (C_V)

Analytical expressions delineate the degenerate (Deg.) and non-degenerate (Non-Deg.) regions as well provide checks on exact numerical calculations.

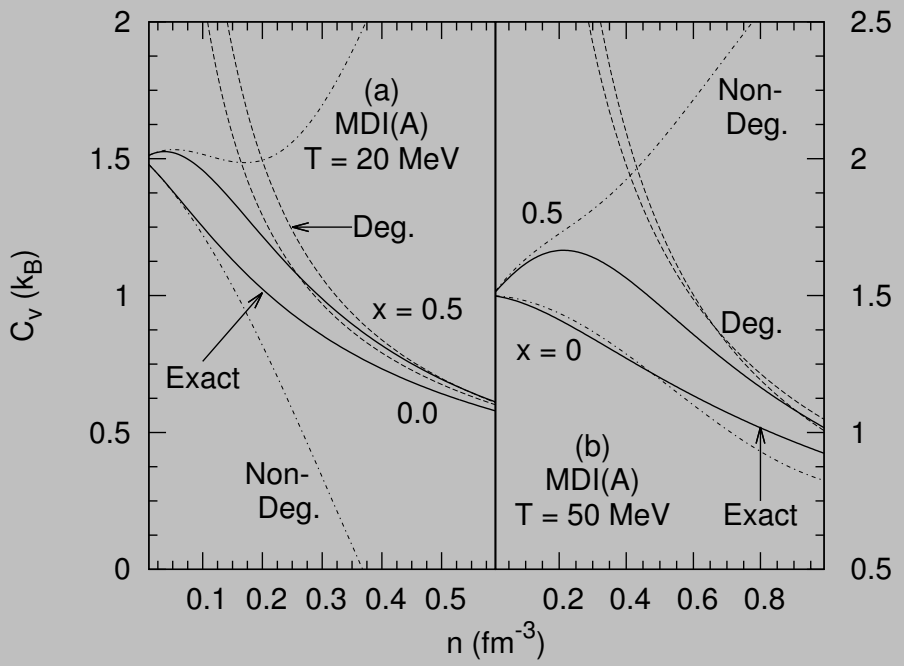

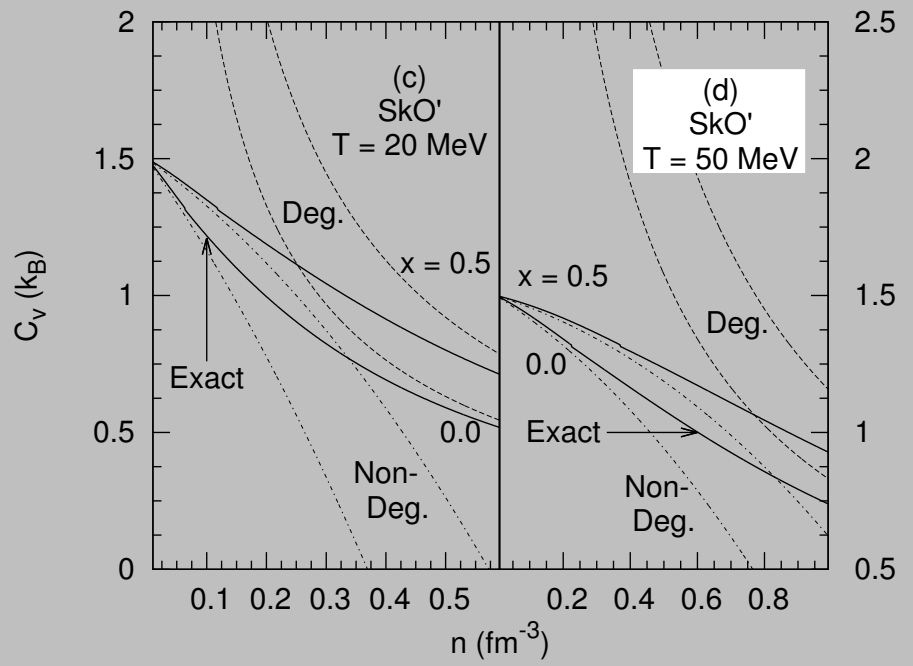

MDI models exhibit a peaks at low n's whereas Skyrme models (e.g., SkO′) do not due to differences in m^*/m's. Quantitative differences are T and x (proton fraction) dependent.

Comparisons in special limits (C_P)

Analytical expressions delineate the degenerate (Deg.) and non-degenerate (Non-Deg.) regions as well provide checks on exact numerical calculations.

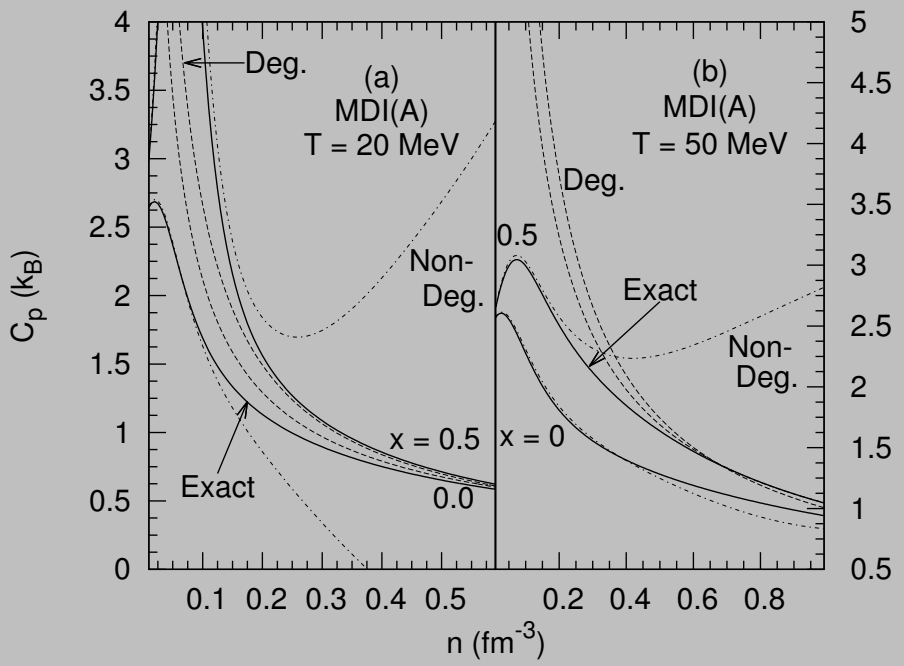

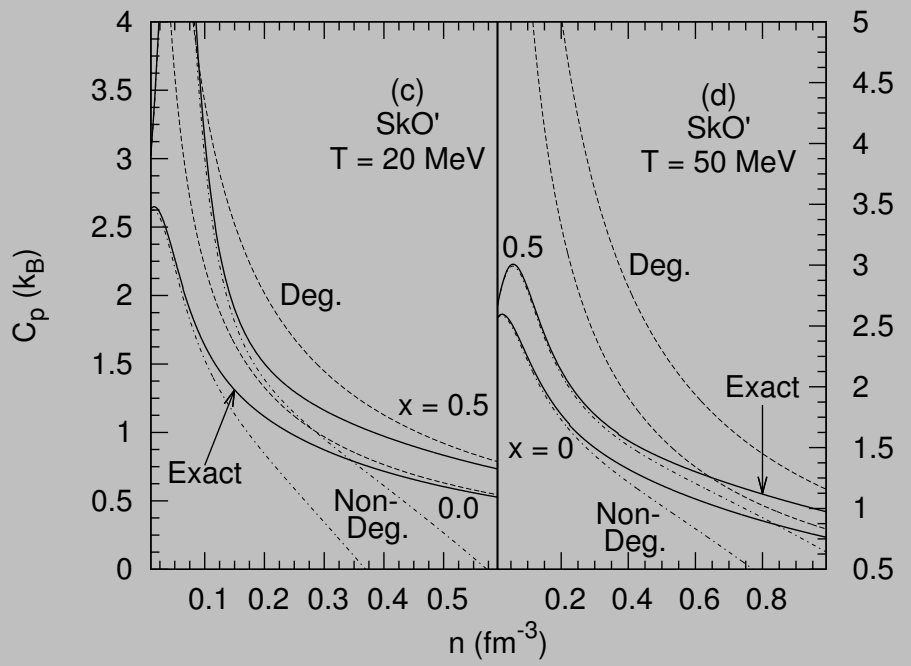

Peaks in C_p are caused by $dP/dn \rightarrow 0$ at sub-saturation densities (the liquid-gas phase transition). Quantitative differences are T and x (proton fraction) dependent.

Degenerate Limit Thermodynamics Beyond Leading Order

C. Constantinos, B. Muccioli, M. Prakash & J.M. Lattimer; ongoing work (2015).

For a general density-dependent $R(p)$, define a p-dependent effective mass as

$$\mathcal{M}(p) = m\left[1 + \frac{m}{p}\frac{dR(p)}{dp}\right]^{-1} .$$

Connection to the Landau effective mass m^* is

$$\mathcal{M}(p = p_F; T = 0) = m^* ,$$

where p_F is the Fermi momentum.

Note:

$$\left.\frac{d\mathcal{M}(p)}{dp}\right|_{p_F} = \mathcal{M}'_F \neq m^{*\prime} = \frac{d\mathcal{M}(p_F)}{dp_F}$$

as R can contain both p and p_F (via n).

Degenerate Limit Thermodynamics Beyond Leading Order

With $a = \pi^2 m^*/(2p_F^2)$, $Q = 1 - \frac{3n}{2m^*}\frac{dm^*}{dn}$, and

$$L_F \equiv \frac{7}{12}p_F^2\frac{\mathcal{M}_F'^2}{m^{*2}} + \frac{7}{12}p_F^2\frac{\mathcal{M}_F''}{m^*} + \frac{3}{4}p_F\frac{\mathcal{M}_F'}{m^*}\,.$$

Entropy per particle:

$$S = 2aT - \frac{16}{5\pi^2}a^3T^3(1 - L_F)$$

Thermal energy:

$$E_{th} = aT^2 - \frac{12}{5\pi^2}a^3T^4(1 - L_F)$$

Thermal pressure:

$$P_{th} = \frac{2}{3}anQT^2 - \frac{8}{5\pi^2}a^3nQT^4\left(1 - L_F + \frac{n}{2Q}\frac{dL_F}{dn}\right)$$

Degenerate Limit Thermodynamics Beyond Leading Order

With $a = \pi^2 m^*/(2p_F^2)$, $Q = 1 - \frac{3n}{2m^*}\frac{dm^*}{dn}$, and

$$L_F \equiv \frac{7}{12}p_F^2\frac{\mathcal{M}_F'^2}{m^{*2}} + \frac{7}{12}p_F^2\frac{\mathcal{M}_F''}{m^*} + \frac{3}{4}p_F\frac{\mathcal{M}_F'}{m^*}\,.$$

Thermal chemical potential:

$$\mu_{th} = -a\left(1 - \frac{2Q}{3}\right)T^2 + \frac{4}{5\pi^2}a^3T^4\left[(1-L_F)(1-2Q) - n\frac{dL_F}{dn}\right]$$

Specific heat at constant volume:

$$C_V = 2aT - \frac{48}{5\pi^2}a^3T^3(1-L_F)$$

Specific heat at constant pressure:

$$C_P = C_V + \frac{16}{9}\frac{a^2Q^2T^3}{\frac{dP_0}{dn}}$$

BLO results for the MDI model - I

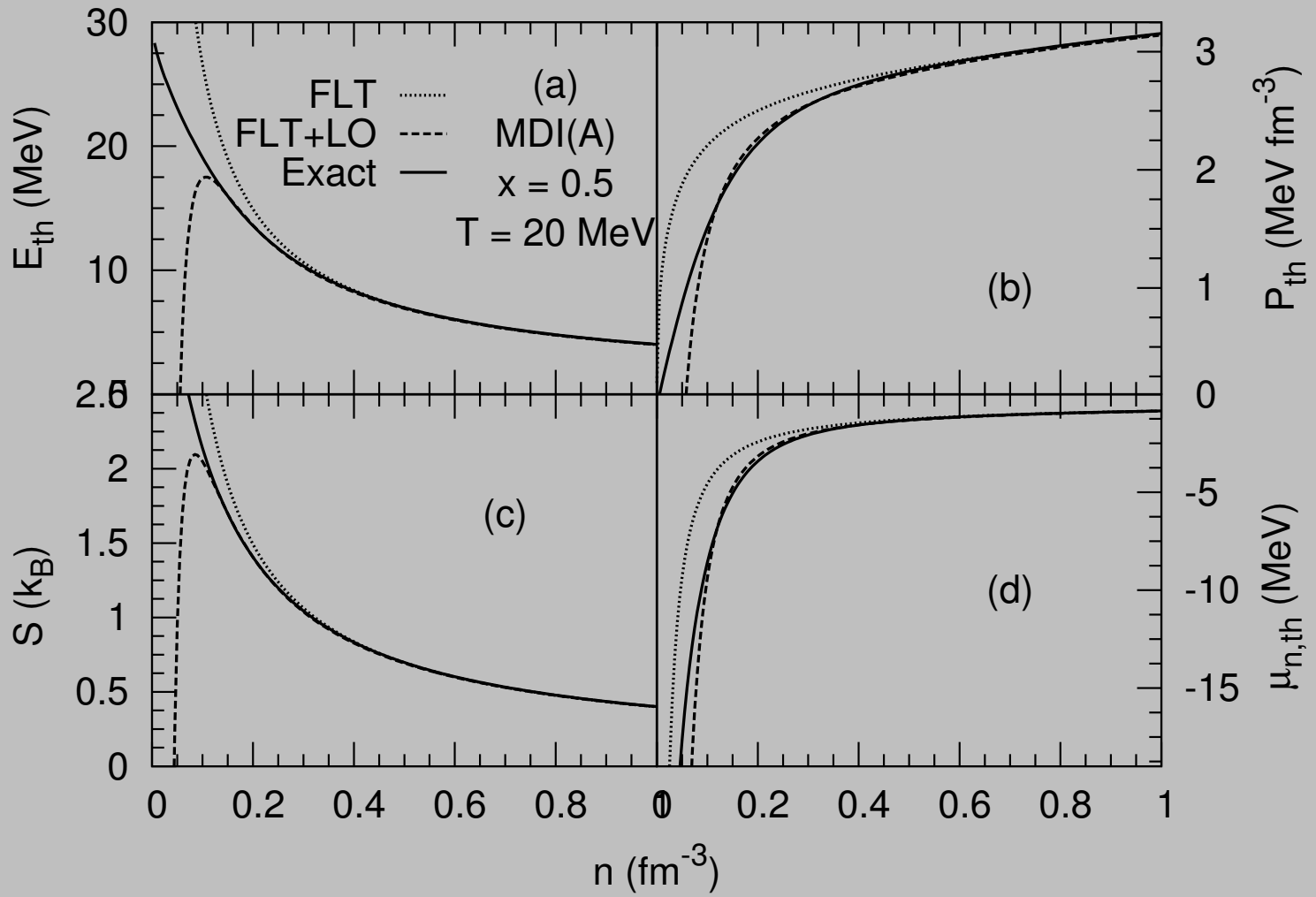

Non-relativistic model with nucleons only. Agreement with the exact results extended to n as low as $\simeq 0.1\ \mathrm{fm}^{-3}$. Similar agreement obtained for matter with $x = 0$.

BLO results for the MDI model - II

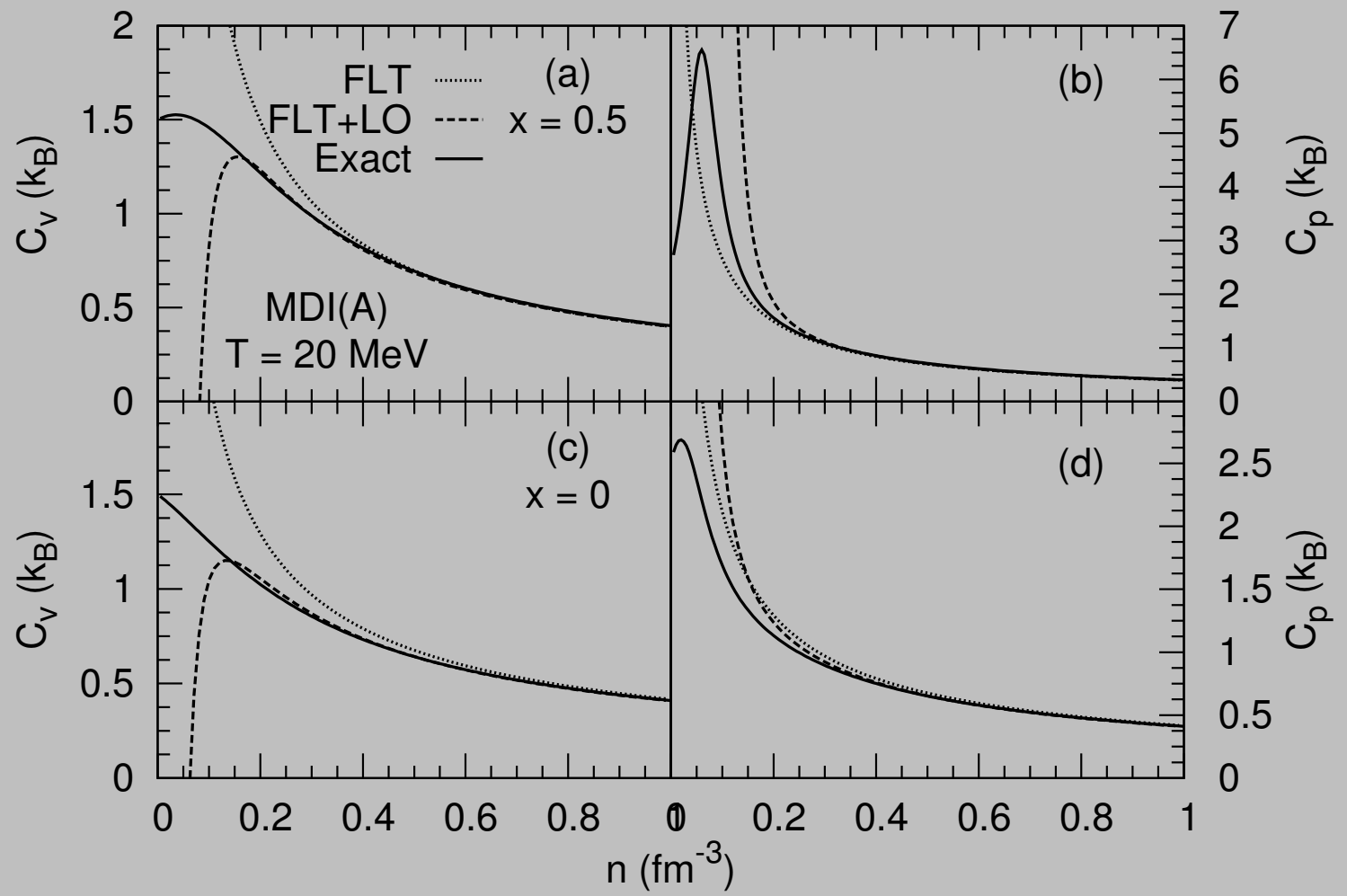

Non-relativistic models with nucleons only. Agreement with the exact results extended to n as low as $\simeq 0.16\ \mathrm{fm}^{-3}$, except for C_p with $x = 0.5$ (lurking liquid gas phase transition).

Beyond relativistic mean field theories (2-loops) - I

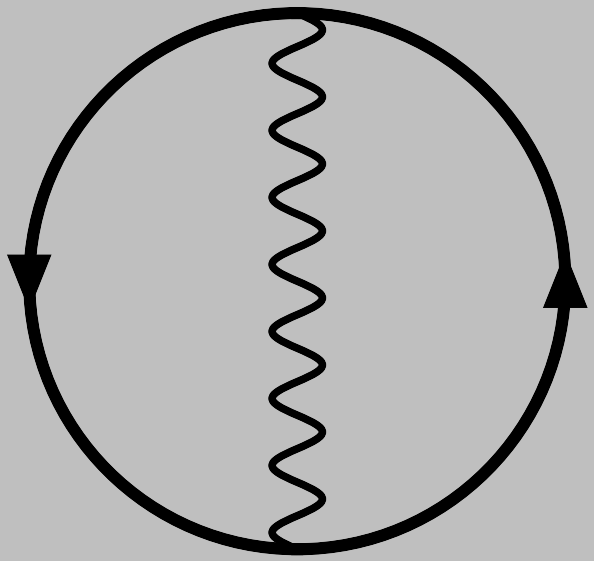

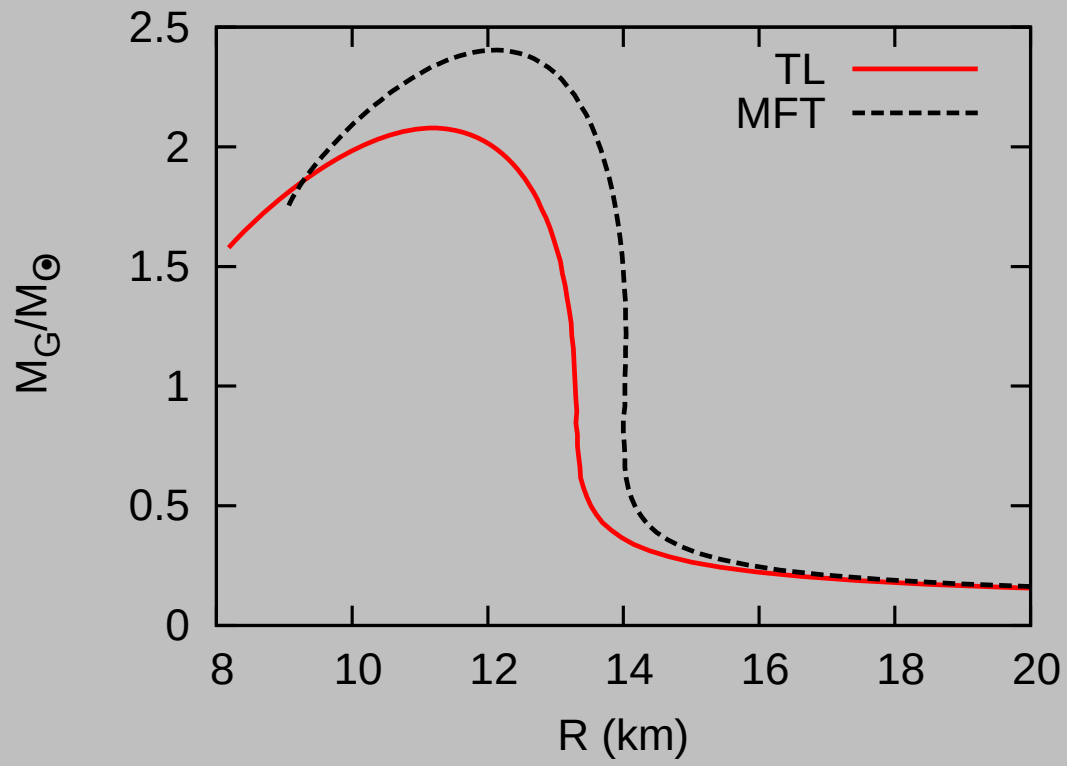

Wavy line indicates exchange of π, σ, ω and ρ mesons.

Xilin-Zhang and M. Prakash (paper in preparation).

Beyond relativistic mean field theories (2-loops) - II

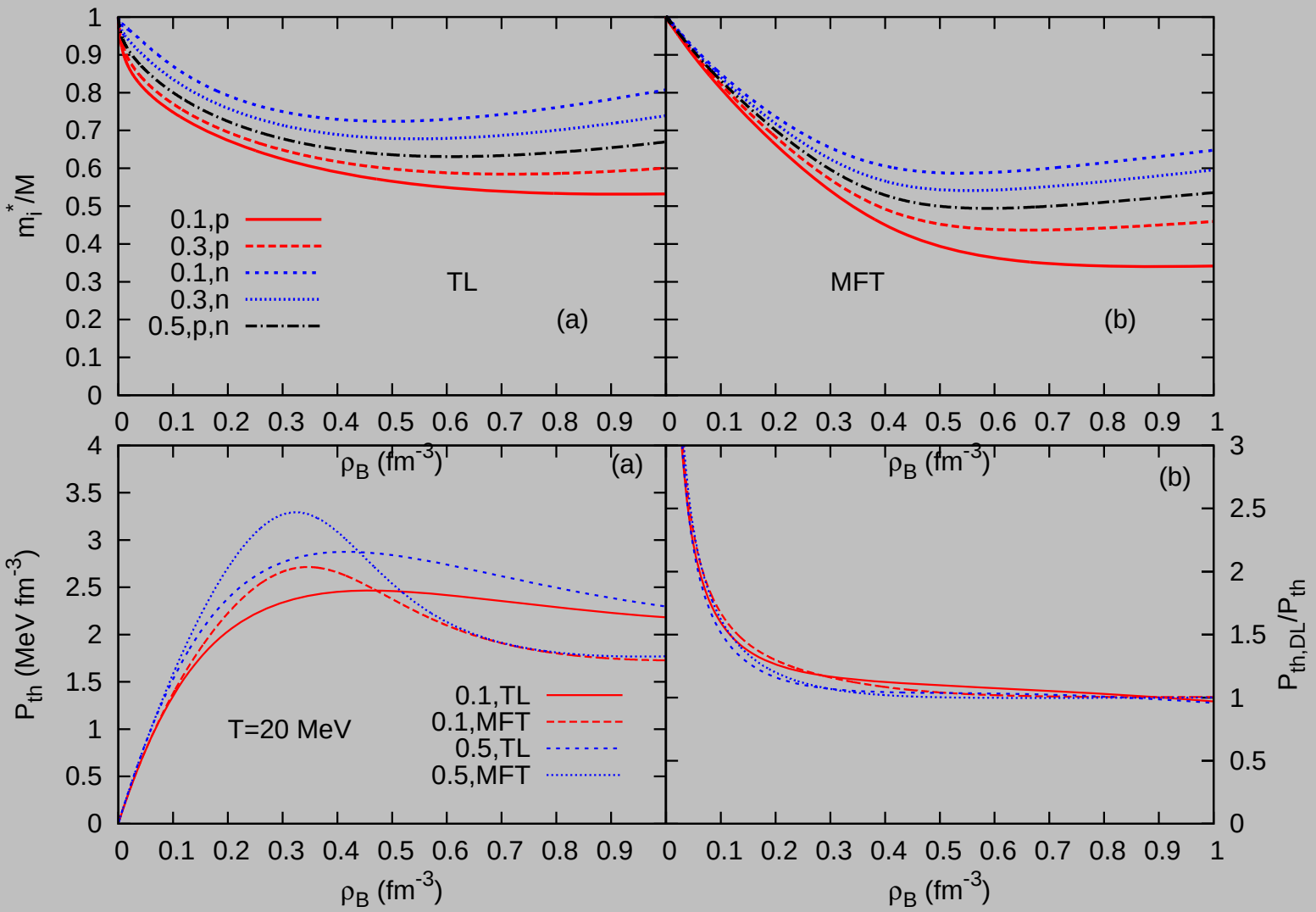

The role of effective masses is similar to those of other models.

Clusters in the inhomogeneous phase

- For densities $n \leq 10^{-3}$ fm^{-3}, and temperatures T not exceeding their $B.E/A$, clusters of light nuclei, such as $\alpha, \mathrm{d}, \mathrm{t},$ *etc.*, are permitted in matter.
- The treatment of clusters is afforded by the viral expansion approach that includes bound and continuum states, and provides corrections to the ideal gas result. When applicable, this approach is model independent as experimental data where available is input to theory.

In terms of the partition function $\mathcal{Q}$, the pressure $P = \frac{T}{V} \log \mathcal{Q}$, and is expressed in terms of the fugacities $z_i = \exp(\mu_i/T)$ (i=N, d, α, *etc.*,) and the 2nd virial coefficients b_2 which are simple integrals involving thermal weights and elastic scattering phase shifts.

Sample references:

E. Beth and G. E. Uhlenbeck, Physica **4** (1937) 915
R. Venugopalan and M. Prakash, Nucl. Phys. A **546** (1992) 718
C. J. Horowitz and A. Schwenk, Nucl. Phys. A **776** (2006) 55
.....

Clusters of light nuclei & their thermal properties

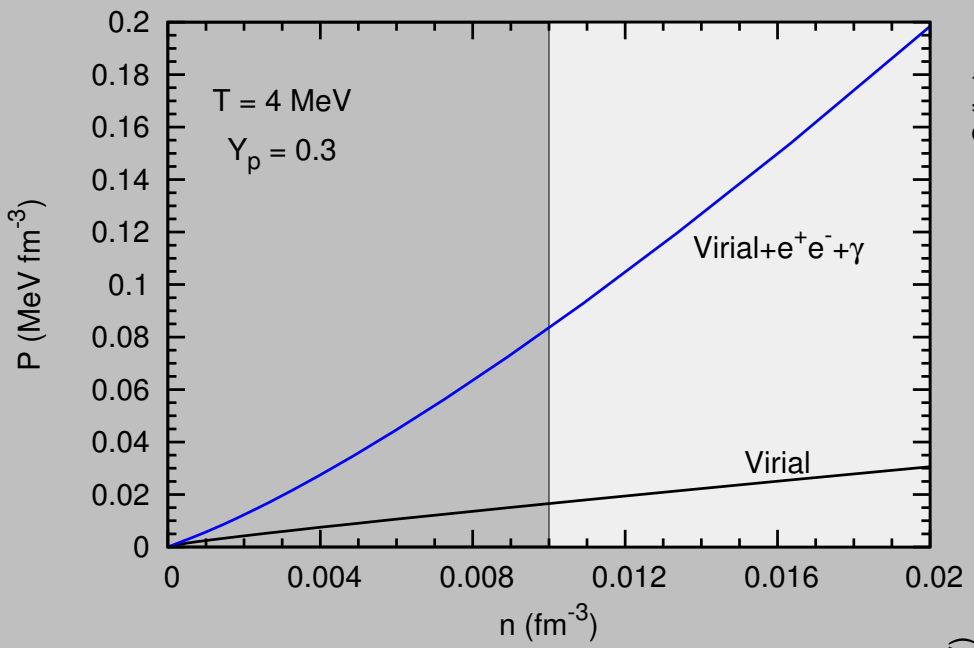

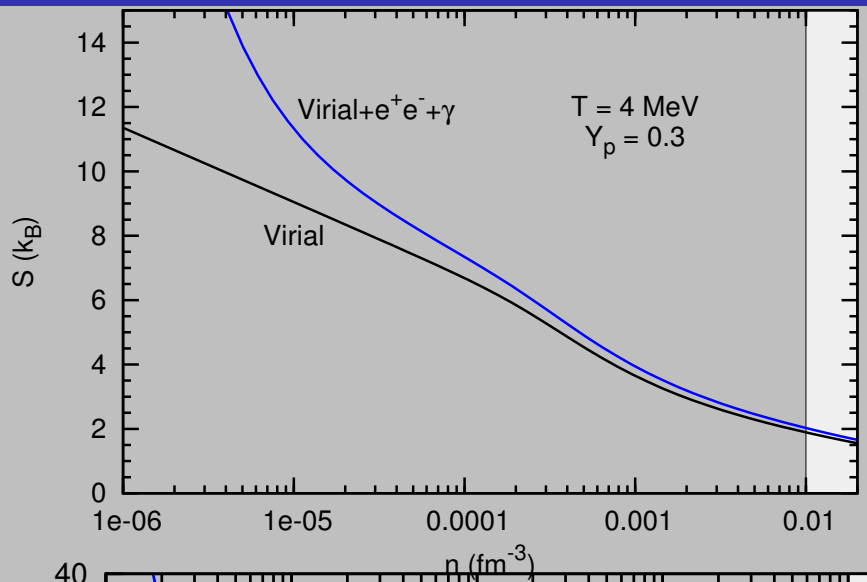

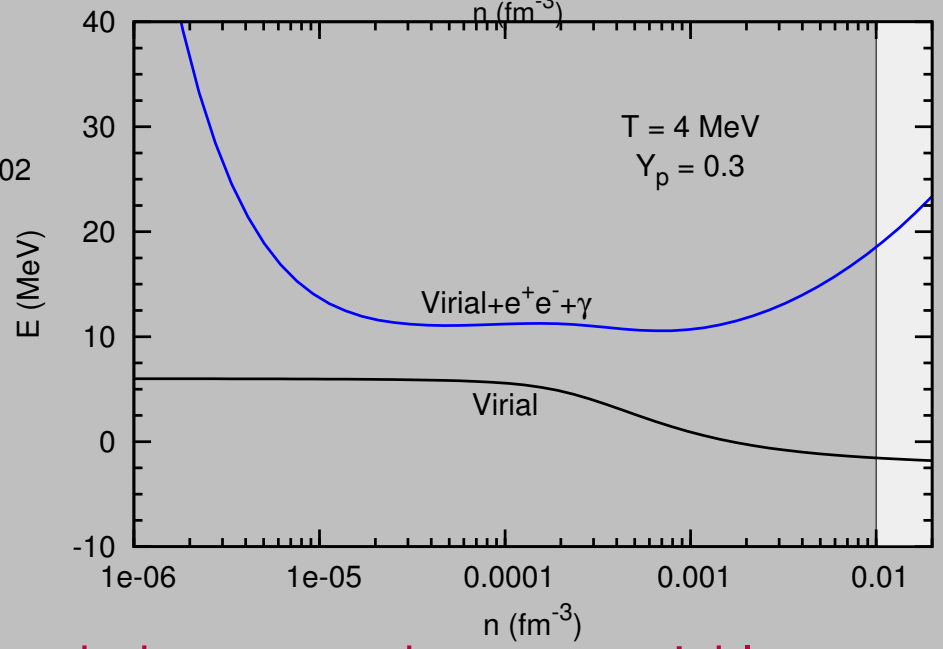

Note the dominant role of leptons and photons on the state variables.

Thermal properties of neutron-rich nuclei

Nucleon effective masses $m^*_{n,p}$ feature prominently in the level density $\rho(E_x)$ of nuclei.

Measured level densities are often "force-fit" to Bethe's formula (1937):

$$\rho(E_x) \propto \frac{1}{E_x^{5/4}} \exp(\sqrt{aE_x}),$$

or, to its back-shifted variant due to Gilbert and Cameron (1965) with

$$E_x \rightarrow E_x - \Delta$$

Above,
E_x: Excitation energy,
$a = \frac{\pi^2 m^*}{2p_F^2}$: the level density parameter, and
Δ: an energy shift due to shell and pairing effects.

Data gathered from (a) Neutron resonances, (b) charged particle resonances, (c) Inelastic scattering and nuclear reactions to resolved levels, and (d) spectrum of evaporated particles.

Nuclei & their level density parameter *a*

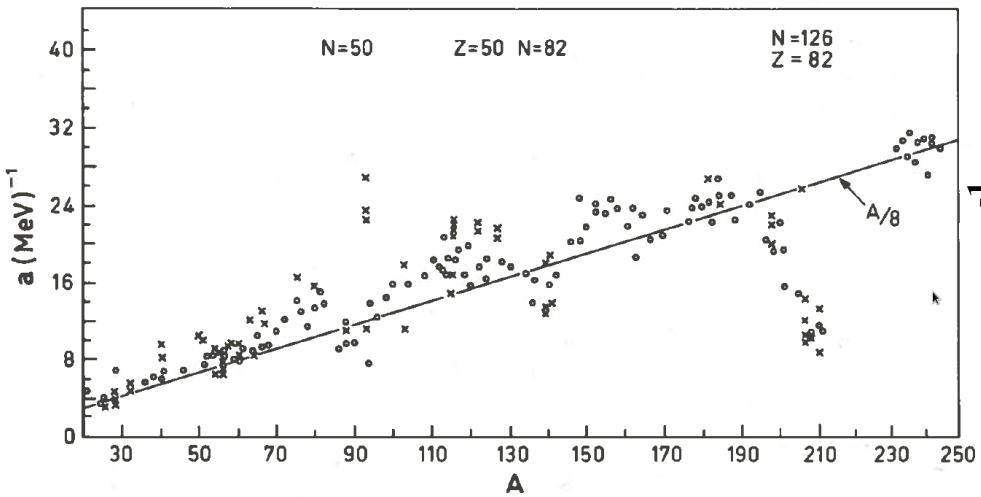

Figure 2-12 The parameter *a* appearing in the Fermi gas level density formula has been determined by comparison with the average spacings observed in slow neutron resonances (values indicated by O), and from evaporation spectra (values indicated by X). The figure is based on the analysis of E. Erba, U. Facchini, and E. Saetta-Menichella, *Nuovo cimento* **22**, 1237 (1961). This analysis also confirms the consistency with direct level counts.

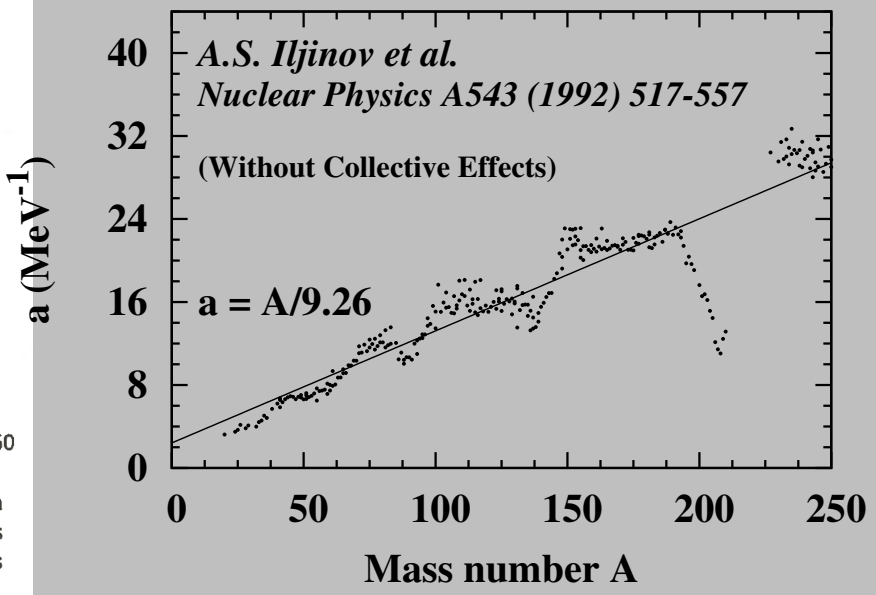

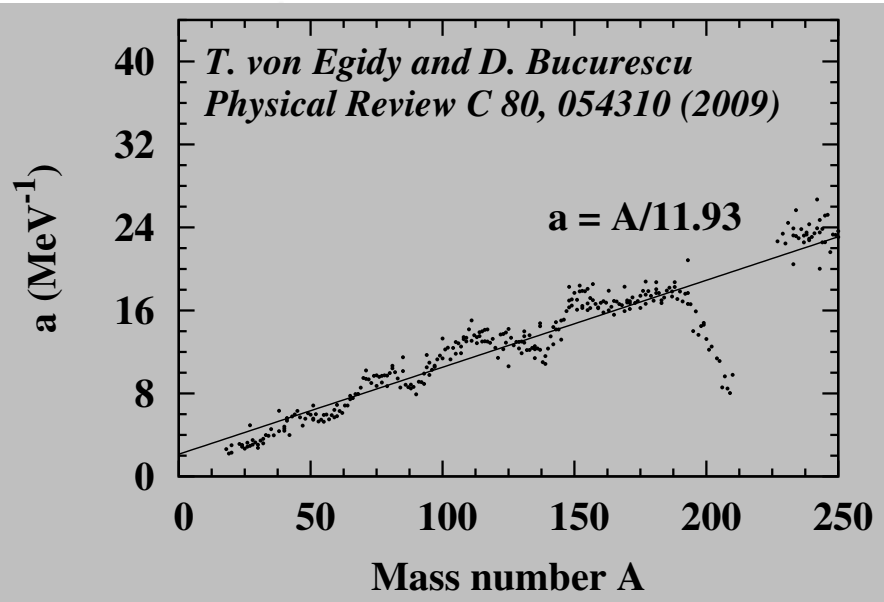

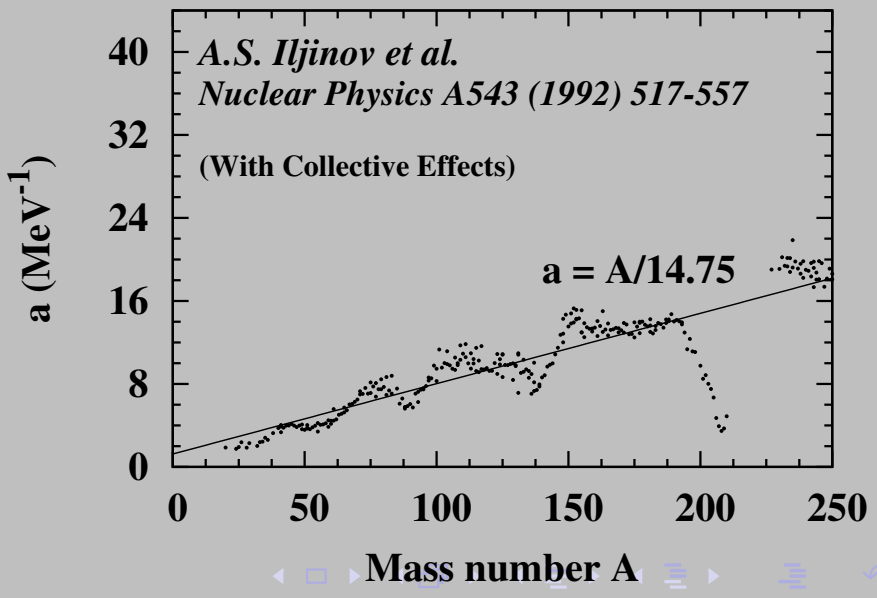

Nuclei and their thermal properties (HFB calculations)

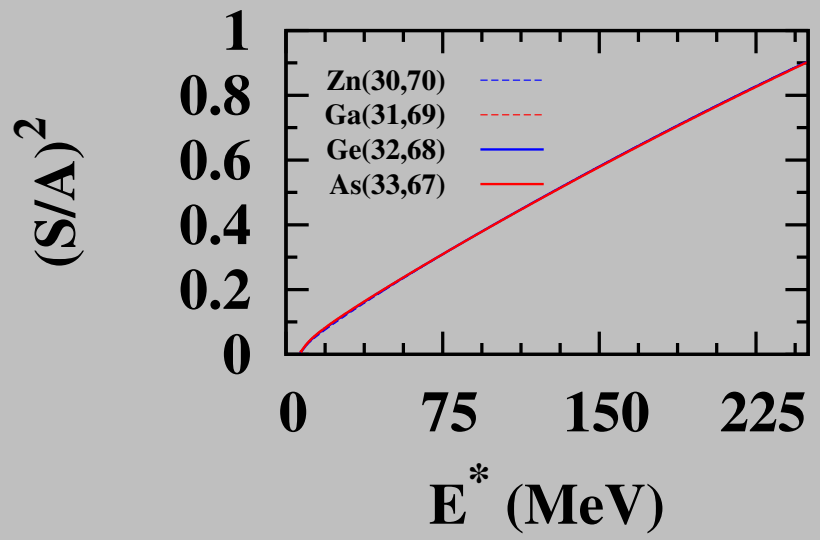

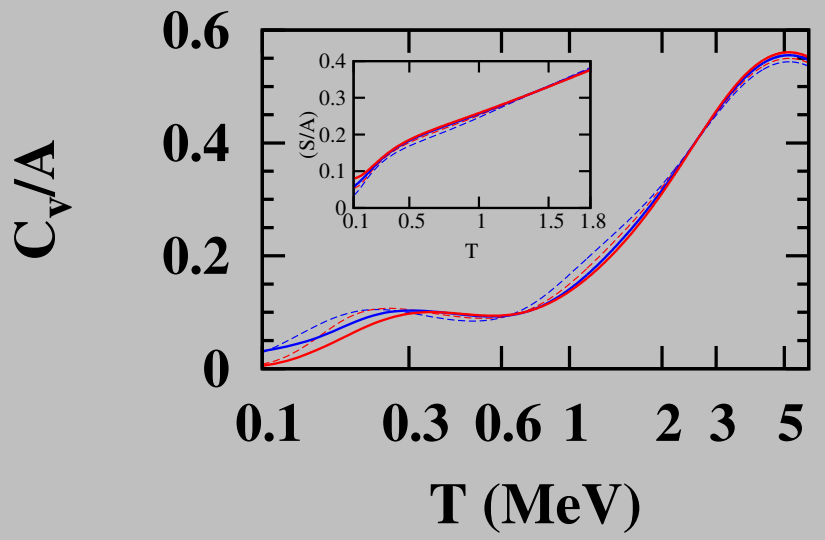

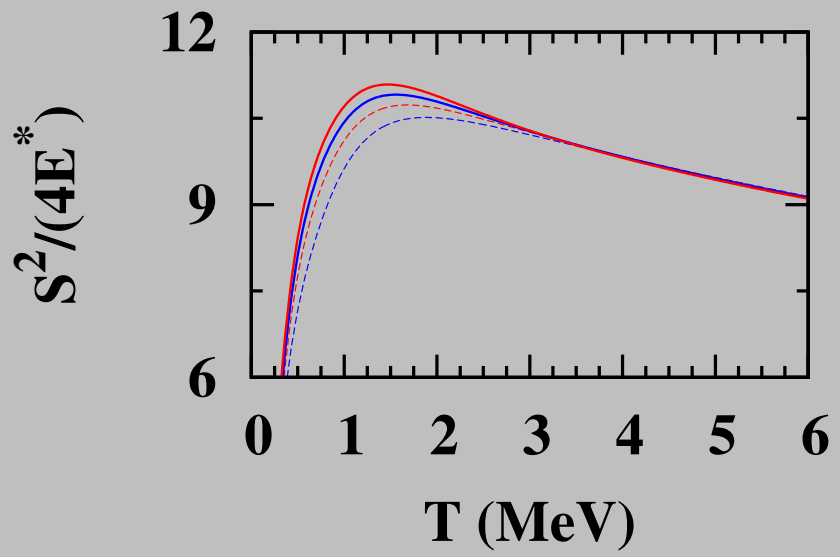

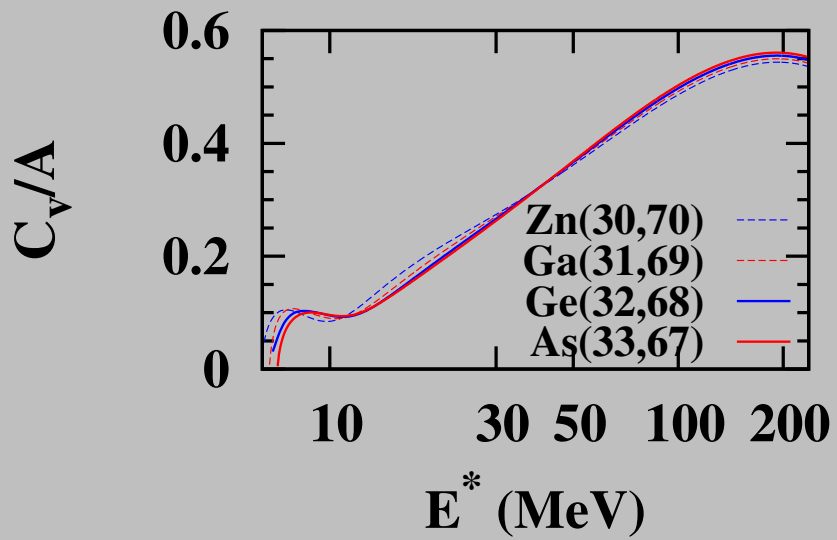

Aspects that deserve further scrutiny

Thermal Properties of Dense Matter: The Inhomogeneous Phase

- How do nuclei respond to heat? Effects of deformation, shell, pairing and collective effects, etc.
- Are theoretical tools in place to pin down the thermal properties of highly neutron-rich nuclei?
- Boiling pasta phases.

Super-nuclear phase transitions at finite S.

For $S \gg 1$, inclusion of other degrees of freedom.